

DOI:10.12158/j.2096-3203.2021.01.028

磷酸铁锂电池模组过充热失控特性及细水雾灭火效果

赵蓝天¹, 金阳¹, 赵智兴¹, 孙磊², 郭东亮², 刘洋²

(1. 郑州大学电气工程学院电网储能与电池应用研究中心, 河南 郑州 450001;

2. 国网江苏省电力有限公司电力科学研究院, 江苏 南京 211103)

摘要:磷酸铁锂电池模组的热失控及灭火是大规模应用急需解决的问题。文中分别以单个磷酸铁锂电池模组和簇级磷酸铁锂电池模组为试验对象,在恒流过充方式下研究单个磷酸铁锂电池模组与簇级磷酸铁锂电池模组的热失控特性,并使用细水雾作为灭火剂,研究细水雾对磷酸铁锂电池模组的灭火效果。试验结果显示:簇级磷酸铁锂电池模组燃烧后温度急剧上升,18 s内温升速率达42.74 °C/s,温度峰值近1 000 °C,明显高于单个模组的峰值温度(600 °C);细水雾持续喷洒100 s后,2组试验模组温度迅速降低,明火完全扑灭无复燃,灭火效果极佳。试验结果可为磷酸铁锂电池储能电站的安全和消防提供有效的理论与试验支撑。

关键词:磷酸铁锂电池;细水雾;过充;热失控;灭火

中图分类号:TM911

文献标志码:A

文章编号:2096-3203(2021)01-0195-06

0 引言

随着电化学与储能技术的不断进步,电池储能技术日益发展并不断完善^[1-7]。在各种锂电池中,磷酸铁锂电池^[8-14]因其能量密度高和可靠安全等特点,不仅可应用于电动汽车行业,在储能电站中也具有很好的发展前景。而实际应用中,磷酸铁锂电池易于过充,电池内部发生化学反应而不断产热,热量聚集,最终导致热失控^[15-19]引起火灾,给储能电站带来巨大的人员与经济损失。文献[20]通过结合多通道电池循环仪和加速量热仪,研究绝热条件下商业化的 $\text{LiCoO}_2 + \text{Li}(\text{Ni}_{0.5}\text{Co}_{0.2}\text{Mn}_{0.3})\text{O}_2/\text{C} + \text{SiO}_x$ 过充期间的动态热行为。结果表明,拐点电压和最大电压随着电流速率的增加而线性增加,电池应在拐点电压后的2 min内采取有效方法来冷却电池,防止热失控。文献[21]以剩余容量为80%的软包磷酸铁锂电池为研究对象,分别对电池在低温和常温循环状态下进行热失控分析,发现低温下电池充放电循环更容易产生锂枝晶,造成化学性质发生不可逆衰退。

针对电池热失控引起的火灾消防问题,我国已研究并试验了多种灭火剂^[22-23]的灭火效果。文献[24]通过对磷酸铁锂电池燃烧特性、火灾危险等级等进行研究,梳理了不同灭火剂灭火效果,为锂离子储能电站的大规模应用提供了有效支持。但上述文献仅局限于单体或是模组级的磷酸铁锂电池热失控及灭火研究,而在储能电站应用中电池是成

簇的^[25],并不能准确、有效反映大规模应用磷酸铁锂电池的储能电站的真实情况。

文中以单个磷酸铁锂电池模组和簇级磷酸铁锂电池模组为试验对象,研究2种级别下磷酸铁锂电池的过充热失控特性及细水雾灭火效果。并采用可见光、热电偶、气体探头等进行实时监测,对比2种级别下温度、产气、电压电流和灭火效果。试验结果表明簇级磷酸铁锂电池模组积热严重,细水雾灭火效果极佳,而 H_2 并非垂直向上扩散,气体预警时需要多点布置。

1 过充热失控及灭火实时监测试验平台

1.1 试验环境

文中模拟真实的电池热失控及细水雾灭火现象,分别采用磷酸铁锂电池模组和簇级磷酸铁锂电池模组搭建真实的试验平台。磷酸铁锂电池模组由32块单体电池四并八串组成,单体额定电压为3.2 V,额定容量为86 A·h,模组额定电压为25.6 V,额定容量为344 A·h,额定电量为8.8 kW·h,四周挡板未拆除,模组加装垂直方向抬高的顶盖,顶盖两侧各有2列错位布置的圆形开孔;簇级磷酸铁锂电池模组由5个上述相同模组组成,呈“十”字分布,充电模组为0号,其他上下左右4个模组分别为2,4,3,1。电池模组和灭火装置具体见图1。

1.2 试验方案

分别以0.5 C,172 A恒流对单个磷酸铁锂电池模组和簇级磷酸铁锂电池模组进行充电,电池发生热失控后,停止过充,启动细水雾进行灭火,并通过可见光、热电偶、气体探头等对模组过充至热失控

收稿日期:2020-08-02;修回日期:2020-09-16

基金项目:国家自然科学基金资助项目(51807180)

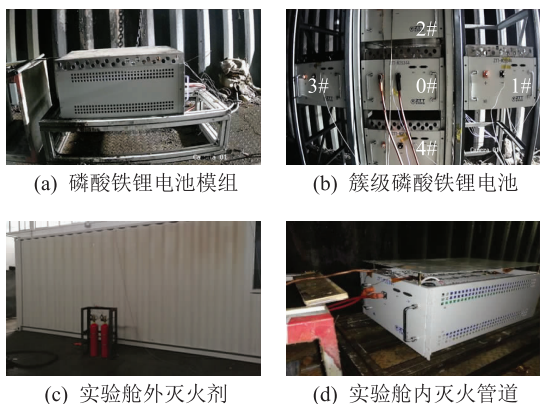
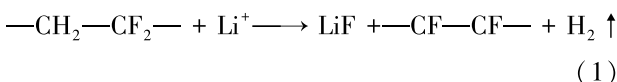


图1 试验环境

Fig.1 Test environment

及灭火过程进行实时监控。

磷酸铁锂电池过充后,内部会产生锂枝晶,电锂枝晶与PVDF反应生成H₂,反应方程式如下:



同时,正极含锂量越来越低,氧化性越来越强,与电解液发生反应,生成CO,方程式如下:



因此,试验中探测到的气体为H₂、CO,故分别在模组正上方0 m,2 m,4 m,6 m处各安置1组H₂、CO探头。单个模组与簇级模组的试验现象不同,单个模组试验中0 m处探测器量程为0~1 000 mg/L,而2 m,4 m,6 m处探测器量程为0~5 000 mg/L;簇级模组试验中CO气体探测器量程均为0~5 000 mg/L,H₂探测器仅2 m处量程为0~5 000 mg/L而0 m,4 m,6 m处氢气探测器量程均为0~1 000 mg/L。

试验中选择中压细水雾(0.2 MPa)作为灭火剂,试验期间远程控制装置启停,将集装箱外的灭火剂通过管道输送到集装箱内,集装箱内铺设的灭火管道正对电池模组,可实现精准快速灭火。

2 试验结果展示

2.1 单个磷酸铁锂电池模组

2.1.1 热失控电压电流及可见光监测

t=0 s时开始过充,电压电流变化见图2,可见光监测的磷酸铁锂电池模组热失控及灭火现象见图3。

如图2所示,过充前期,模组电压增大至额定电压1.6倍后趋于平缓;1 770 s后浓烟冒出,而电池内部锂枝晶熔断,短路点被高温烧断,电压下降过程中出现抬升;浓烟扩散后,模组电压开始急剧下降,至2 219 s模组起火。

图3中,过充1 181 s时,首个安全阀打开,电解

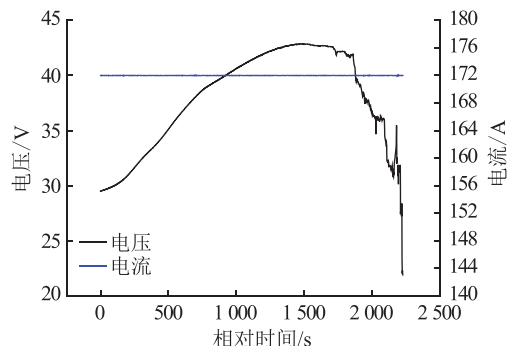


图2 磷酸铁锂电池模组电压和电流

Fig.2 Voltage and current variation of lithium iron phosphate battery module

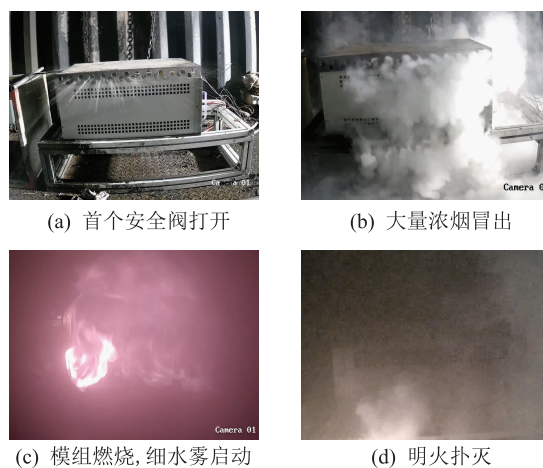


图3 磷酸铁锂电池模组可见光监测

Fig.3 Visible light monitoring diagram of lithium iron phosphate battery module

液喷出,此后几分钟内安全阀陆续打开;1 770 s后,大量浓烟冒出,逐渐弥漫整个储能舱;2 219 s时模组出现明火,剧烈燃烧,立即启动细水雾进行灭火;2 364 s时在细水雾的持续喷射下,明火完全扑灭,无复燃现象。

2.1.2 热失控温度及产气监测

在磷酸铁锂电池模组热失控及灭火过程中,热电偶对模组上表面T₁和模组中心T₂监测见图4,气体检测见图5。

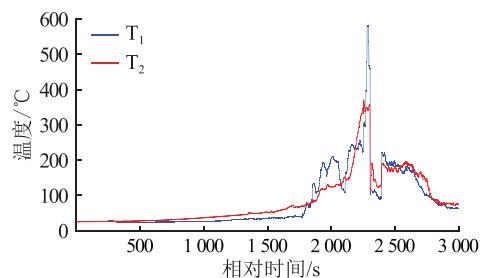


图4 热电偶温度监测

Fig.4 Temperature monitoring diagram of thermocouple

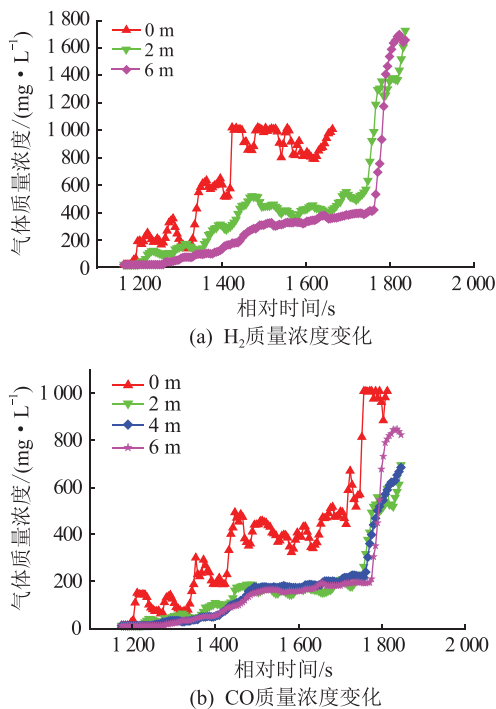


图5 磷酸铁锂电池模组气体检测

Fig.5 Gas detection diagram of lithium iron phosphate battery module

由图4可看出,前期模组各测点温度较均匀上升,在1770s冒浓烟时中心温度约100℃。此后烟气逐渐弥漫,温升速率加快,但过程中存在波动。2219s起火后,上表面温度峰值达到600℃。出现明火时立即启动细水雾,模组温度迅速下降,2364s时明火完全熄灭,上表面温度下降到102.6℃,继续喷洒至2819s,10min内模组温度持续下降,未出现复燃现象。

图5(a)中,4m处H₂探头损坏,首个安全阀打开后(1181s),0m处探测器在1201s监测到H₂含量提升;2m处探测器在1221s监测到H₂气体含量变化,6m处H₂探测器于1286s监测到H₂含量提升。图5(b)中,0m处探测器在1206s探测到CO含量提升;1236s时2m处探测到气体质量浓度提升;4m和6m处CO探测器分别于1261s和1296s监测到CO含量的提升。试验中后期随着气体逐渐由近及远扩散,0m处H₂质量浓度后期超出量程不再显示,其他3组探测器监测到的H₂、CO含量变化趋势基本相同,且数值相差较小。

2.2 簇级磷酸铁锂电池模组

2.2.1 热失控电压电流及可见光监测

$t=0$ s时开始过充,监测到的电压电流变化见图6,可见光监测的簇级磷酸铁锂电池模组热失控及灭火现象见图7。

由图6可知,过充前期,模组电压逐渐增大至额

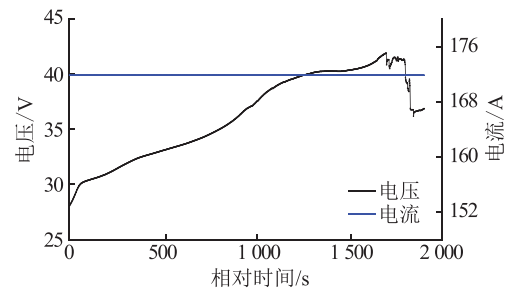


图6 簇级磷酸铁锂电池模组电压和电流

Fig.6 Voltage and current monitoring diagram of clustered lithium iron phosphate battery

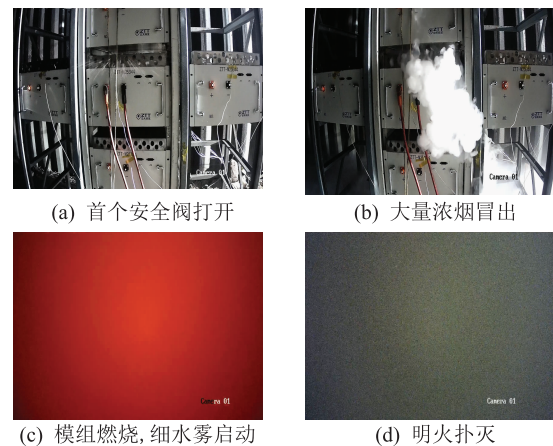


图7 簇级磷酸铁锂电池模组可见光监测

Fig.7 Visible light monitoring diagram of cluster lithium iron phosphate battery

定电压1.6倍后趋于平缓;1715s浓烟冒出前后,电池内部锂枝晶熔断,短路点被高温烧断,电压略微抬升;浓烟弥漫后,模组电压急剧下降,至1952s模组起火。

图7中模组过充1015s时,随着模组电压提高,气体和热量积聚在过充模组内部,压力不断增大,冲破安全阀,首个安全阀打开,电解液喷出,随后安全阀陆续打开;1715s后,随电池内部反应进行,大量浓烟冒出,向四周扩散;1952s时模组出现明火,剧烈燃烧,立即启动细水雾进行灭火;细水雾的持续喷射下,至2068s明火完全扑灭,无复燃现象。

2.2.2 热失控温度及产气监测

在整个簇级磷酸铁锂电池模组热失控及灭火过程中,热电偶温度监测见图8,气体检测见图9。

图8(a)中,0号电池模组后侧和左侧的温度变化特性相似,1952s明火出现,模组后侧温度迅速上升,最高温度至942.7℃,2068s细水雾灭火后,左后两侧温度快速下降,后侧温度下降为83.4℃,但电池内部仍有反应,所以温度存在波动性;图8(b)中,2号模组中心温度明显比左侧温度高,4号

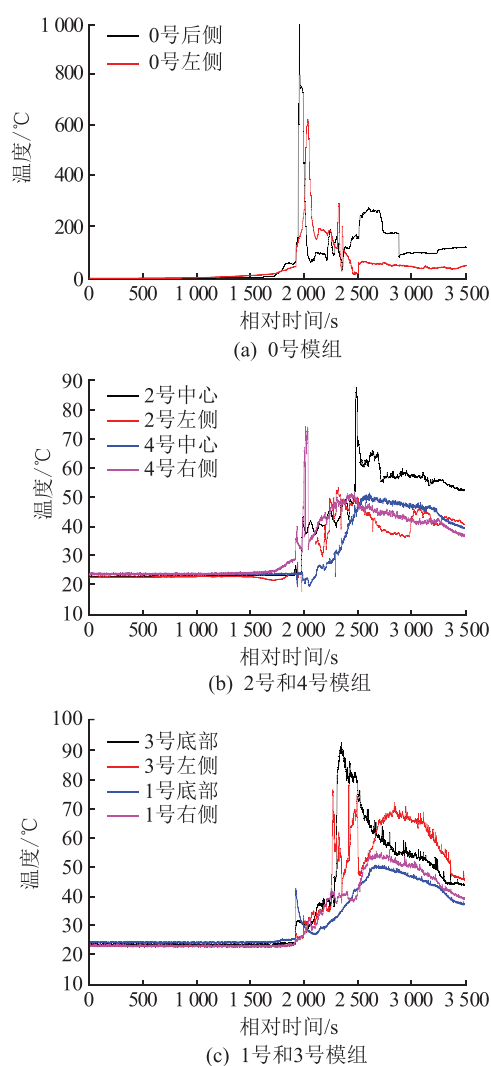


图8 簇级磷酸铁锂电池模组热电偶温度检测
Fig.8 Temperature detection diagram of thermocouple of cluster lithium iron phosphate battery module

模组模组右侧温度明显高于中心温度,而整体上2号模组温度高于4号模组,这是由于出现明火后,燃烧的火焰给上面的模组加热;图8(c)中,分别位于充电模组的左右两侧的3号模组和1号模组,明火出现前各部分温度基本不变,明火出现后1号模组右侧和3号模组底部温度较其他部位高,同时3号模组的温度整体比1号模组温度高;从5个模组整体上看,各模组在产生明火后温度均大幅度提升,1952 s明火出现后,立即启动细水雾并持续喷洒至2852 s,15 min后温度迅速降低,细水雾灭火具有很好的灭火效果。

由图9(a)可知,2 m处H₂探测器首先检测出H₂,是因为2 m处使用的探测器量程更大,更加灵敏。在监测H₂含量的过程中,所测得浓度存在波动,但2 m处气体探测器测得H₂质量浓度持续最高;图9(b)中,6 m处探测器损坏,首个安全阀

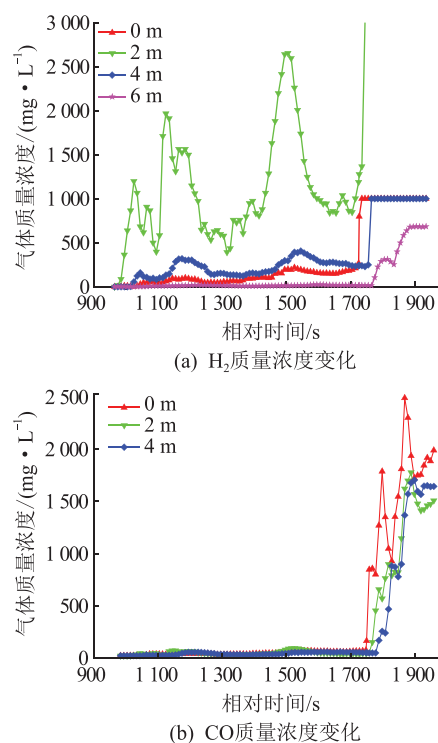


图9 簇级磷酸铁锂电池模组气体检测
Fig.9 Gas detection diagram of cluster lithium iron phosphate battery module

(1015 s)打开后监测到CO气体含量都很低,直至1715 s冒烟阶段,CO含量显著提升,0 m处探测器测得CO含量最高,4 m处探测器测得CO含量最低。

3 对比分析

文中研究了单个磷酸铁锂电池模组与簇级磷酸铁锂电池模组的热失控特性与细水雾灭火效果。

(1) 热失控温度特性。磷酸铁锂电池过充后,温度随着内部化学反应的进行而逐渐升高,热量不断积累,最终发生热失控。簇级磷酸铁锂电池模组0号模组燃烧后18 s内,最高温度由173.3 °C急剧攀升至942.7 °C,温升速率为42.74 °C/s;而单个磷酸铁锂电池模组燃烧后44 s内,温度由234.2 °C攀升至600 °C,温升速率为8.31 °C/s。可见簇级磷酸铁锂电池模组受空间影响,无法很好地散热,使得电池内部的温度急剧升高,远大于单个磷酸铁锂电池模组发生热失控时内部聚集的热量。同时由于热传递效应的存在,会对周围模组产生不同的影响,从温度分布记录上可以看出,周围模组中温度变化最明显的是位于过充模组正上方的模组,这与高温烟气及燃烧时热量向上传播有关,其余模组上测点最高温度普遍小于150 °C,说明及时的降温灭火能有效阻止火灾蔓延。

(2) 热失控气体特性。单个磷酸铁锂电池模组过充后,0 m 处探测器最先探测到气体浓度变化,然后依次是 2 m,4 m,6 m 处气体浓度改变,特征气体呈现明显的由近及远扩散的规律,距离过充模组越近,能够越早探测到对应气体含量的提升,且相同时刻下,距离模组越近气体浓度越高。而簇级磷酸铁锂电池模组过充后,特征气体的扩散规律不尽相同,2 m 处探测器首先探测到气体浓度变化,然后依次是 4 m,0 m,6 m 处探测器,说明该环境下 H_2 的扩散并非垂直向上,故在真实储能舱内进行消防预警时需要多点布置,并提高探测器精准度。

(3) 细水雾灭火特性,具体灭火效果对比见表 1。可知,在 2 次试验中,模组燃烧后,细水雾都可以在短时间内有效扑灭电池火灾,但由于电池内部仍存在化学反应,温度出现回升,且簇级磷酸铁锂电池模组散热差积热严重,故回升温度相较于单个磷酸铁锂电池模组更高。此后细水雾持续喷射,温度持续下降,且无复燃现象出现,具有极好的电池降温 and 阻止复燃的效果。

表 1 细水雾灭火效果对比

Table 1 Comparison of fire extinguishing effect of water mist

模组	是否灭火	灭火时间/s	是否复燃	降温速率/ ($^{\circ}C \cdot s^{-1}$)
单个磷酸铁锂电池模组	是	145	否	3.43
簇级磷酸铁锂电池模组	是	116	否	7.41

4 结语

文中研究了单个磷酸铁锂电池模组与簇级磷酸铁锂电池模组的过充热失控特性及细水雾灭火效果,揭示了真实储能电站中簇级磷酸铁锂电池模组的热失控特性,并以单个电池模组与簇级电池模组的温度热失控差异和气体扩散特性为依托,为储能电站中电池模组的空间布局和气体预警探测器的多点布置提供了可靠的理论与试验依据,同时验证了细水雾持续喷射对簇级磷酸铁锂电池模组灭火的有效性。

随着储能电站的进一步发展,下一步应更加注重对电池模组热失控多点气体预警以及灭火剂和灭火效果的研究,避免大规模火灾事故的发生。

参考文献:

[1] 吴霜,季聪,孙国强. 含分布式储能的配电网多目标运行优化策略研究[J]. 电力工程技术,2018,37(2):20-26.
WU Shuang,JI Cong,SUN Guoqiang. Multiple objection opera-

tion strategy optimization research of distribution network including distributed energy storage[J]. Electric Power Engineering Technology,2018,37(2):20-26.

- [2] 于昌海,吴继平,杨海晶,等. 规模化储能系统参与电网调频的控制策略研究[J]. 电力工程技术,2019,38(4):68-73,105.
YU Changhai,WU Jiping,YANG Haijing, et al. Research on control strategy of large-scale energy storage system participating in power grid frequency modulation[J]. Electric Power Engineering Technology,2019,38(4):68-73,105.
- [3] 刘大贺,韩晓娟,李建林. 基于光伏电站场景下的梯次电池储能经济性分析[J]. 电力工程技术,2017,36(6):27-31,77.
LIU Dahe,HAN Xiaojuan,LI Jianlin. Energy storage economy analysis of cascade cells based on photovoltaic power station scenario[J]. Electric Power Engineering Technology,2017,36(6):27-31,77.
- [4] 葛维春,滕健伊,潘超,等. 含风光储能源储荷规划与运行调控策略[J]. 电力系统保护与控制,2019,47(13):46-53.
GE Weichun,TENG Jianyi,PAN Chao, et al. Operation regulation strategy of source-storage-load with wind energy storage energy[J]. Power System Protection and Control,2019,47(13):46-53.
- [5] 伍惠斌,王淳,左远龙,等. 基于分时电价和蓄电池实时控制策略的家庭能量系统优化[J]. 电力系统保护与控制,2019,47(19):23-30.
WU Huicheng,WANG Chun,ZUO Yuanlong, et al. Home energy system optimization based on time-of-use price and real-time control strategy of battery [J]. Power System Protection and Control,2019,47(19):23-30.
- [6] 李建林,马会萌,惠东. 储能技术融合分布式可再生能源的现状与发展趋势[J]. 电工技术学报,2016,31(14):1-10,20.
LI Jianlin,MA Huimeng,HUI Dong. Present development condition and trends of energy storage technology in the integration of distributed renewable energy[J]. Transactions of China Electrotechnical Society,2016,31(14):1-10,20.
- [7] 姜欣,郑雪媛,胡国宝,等. 市场机制下面向电网的储能系统优化配置[J]. 电工技术学报,2019,34(21):4601-4610.
JIANG Xin,ZHENG Xueyuan,HU Guobao, et al. Optimization of battery energy storage system locating and sizing for the grid under the market mechanism[J]. Transactions of China Electrotechnical Society,2019,34(21):4601-4610.
- [8] 张阳. 磷酸铁锂正极材料的制备与改性研究[D]. 西安:西安建筑科技大学,2017.
ZHANG Yang. Preparation and modification study of $LiFePO_4$ cathode material [D]. Xi'an: Xi'an University of Architecture and Technology,2017.
- [9] 胡华冲. $LiFePO_4/Li_4Ti_5O_{12}$ 电池的研究[D]. 哈尔滨:哈尔滨工程大学,2013.
HU Huachong. Study on $LiFePO_4/Li_4Ti_5O_{12}$ battery [D]. Harbin: Harbin Engineering University,2013.
- [10] 谭义勇. 浅析磷酸铁锂电池[J]. 信息记录材料,2019,20(6):50-51.

- TAN Yiyong. Brief analysis of lithium iron phosphate battery [J]. Information Recording Materials, 2019, 20(6): 50-51.
- [11] BI Haijun, ZHU Huabing, ZU Lei, et al. A new model of trajectory in eddy current separation for recovering spent lithium iron phosphate batteries [J]. Waste Management, 2019(100): 1-9.
- [12] 刘俊华, 张启超, 李程, 等. 磷酸铁锂电池模组健康度快速评估方法研究 [J]. 电网与清洁能源, 2020, 36(10): 112-118.
LIU Junhua, ZHANG Qichao, LI Cheng, et al. Research on the rapid assessment method of the health of lithium iron phosphate battery modules [J]. Power System and Clean Energy, 2020, 36(10): 112-118.
- [13] LIU Shuaihua, LIU Xunliang, DOU Ruifeng, et al. Experimental and simulation study on thermal characteristics of 18650 lithium-iron-phosphate battery with and without spot-welding tabs [J]. Applied Thermal Engineering, 2020(166): 114648.
- [14] LIU Kang, TAN Quanyin, LIU Lili, et al. Acid-free and selective extraction of lithium from spent lithium iron phosphate batteries via a mechanochemically induced isomorphic substitution [J]. Environmental Science & Technology, 2019, 53(16): 9781-9788.
- [15] 崔志仙, 王青松, 孙金华. 锂枝晶导致的锂离子电池内短路模拟研究 [J]. 火灾科学, 2019, 28(2): 101-112.
CUI Zhixian, WANG Qingsong, SUN Jinhua. Numerical study on lithium dendrite-induced internal short circuit of lithium ion battery [J]. Fire Safety Science, 2019, 28(2): 101-112.
- [16] 刘全义, 韩旭, 孙中正, 等. 不同环境体系下锂离子电池热失控特性实验研究 [J]. 安全, 2019, 40(4): 42-46.
LIU Quanyi, HAN Xu, SUN Zhongzheng, et al. Experimental study on thermal runaway of lithium ion battery under different environmental systems [J]. Safety and Security, 2019, 40(4): 42-46.
- [17] LIU Jialong, DUAN Qiangling, MA Mina, et al. Aging mechanisms and thermal stability of aged commercial 18650 lithium ion battery induced by slight overcharging cycling [J]. Journal of Power Sources, 2020(445): 1-9.
- [18] 王文和, 何腾飞, 米红甫, 等. 18650 型锂离子电池燃烧特性及火灾危险性评估 [J]. 安全与环境学报, 2019, 19(3): 729-736.
WANG Wenhe, HE Tengfei, MI Hongfu, et al. Experimental test for the combustion features of the 18650-type lithium ion battery and its fire-prone risk assessment [J]. Journal of Safety and Environment, 2019, 19(3): 729-736.
- [19] 赵梦迪. 动力电池热安全应对及其过热临界行为特征研究 [D]. 吉林: 吉林大学, 2019.
ZHAO Mengdi. Research on thermal safety management and critical overheating behavior for power batteries [D]. Jilin: Jilin University, 2019.
- [20] YE Jiana, CHEN Haodong, WANG Qingsong, et al. Thermal behavior and failure mechanism of lithium ion cells during overcharge under adiabatic conditions [J]. Applied Energy, 2016(182): 464-474.
- [21] 王绥军, 傅凯, 官亦标, 等. 软包磷酸铁锂电池低温热安全性能研究 [J]. 储能科学与技术, 2016, 5(2): 204-209.
WANG Suijun, FU Kai, GUAN Yibiao, et al. Low temperature thermal safety performance of soft packaged lithium iron phosphate battery [J]. Energy Storage Science and Technology, 2016, 5(2): 204-209.
- [22] 张磊, 张永丰, 黄昊, 等. 热过载锂电池失控特性及其早期探测模式研究 [J]. 消防科学与技术, 2018, 37(1): 55-58.
ZHANG Lei, ZHANG Yongfeng, HUANG Hao, et al. Study on the lithium battery thermal runaway characteristics under overheating and the detection mode on battery fires [J]. Fire science and technology, 2018, 37(1): 55-58.
- [23] 黎可, 王青松, 孙金华. 基于火探管式的锂离子电池灭火技术研究 [J]. 火灾科学, 2018, 27(2): 124-131.
LI Ke, WANG Qingsong, SUN Jinhua. Development of fire suppression technology for lithium ion batteries based on fire detection pipe [J]. Fire Safety Science, 2018, 27(2): 124-131.
- [24] 吴静云, 黄峥, 郭鹏宇. 储能用磷酸铁锂 (LFP) 电池消防技术研究进展 [J]. 储能科学与技术, 2019, 8(3): 495-499.
WU Jingyun, HUANG Zheng, GUO Pengyu. Research progress on fire protection technology of LFP lithium ion battery used in energy storage power station [J]. Energy Storage Science and Technology, 2019, 8(3): 495-499.
- [25] 彭志强, 卜强生, 袁宇波, 等. 电网侧储能电站监控系统体系架构及关键技术 [J]. 电力系统保护与控制, 2020, 48(10): 61-70.
PENG Zhiqiang, BU Qiangsheng, YUAN Yubo, et al. Architecture and key technologies of a monitoring and control system for an energy storage power station [J]. Power System Protection and Control, 2020, 48(10): 61-70.

作者简介:



赵蓝天

赵蓝天 (1996), 男, 硕士在读, 研究方向为电网规模化储能技术, 电化学储能电站安全性 (E-mail: 1776291160@qq.com);

金阳 (1989), 男, 博士, 副教授, 研究方向为电网规模化储能技术, 电化学储能电站安全性;

赵智兴 (1997), 男, 硕士在读, 研究方向为电网规模化储能技术, 电化学储能电站安全性。

Circulation and loss calculation model of high voltage GIS shell

ZHAO Yisong¹, SONG Chengwei², XING Kai³, LIU Xinran⁴, WANG Feiming¹, LANG Fucheng¹

(1. State Grid Liaoning Electric Power Co., Ltd. Research Institute, Shenyang 110006, China;

2. Testing and Certification Center of Liaoning Provincial Inspection, Shenyang 110006, China;

3. Shenyang Power Supply Company of State Grid Liaoning Electric Power Co., Ltd., Shenyang 110006, China;

4. State Grid Liaoning Electric Power Co., Ltd. Marketing Service Center, Shenyang 110006, China)

Abstract: High-voltage gas insulate switchgear (GIS) shell circulation is the main cause of operating losses in substations. Circulation can cause the device to heat up. If the substation is operated for a long time, the transmission capacity of the power system and the insulation performance of the equipment will be seriously affected. The purpose of this article is to simplify the loss calculation procedure and improve the calculation accuracy of GIS shell circulation and the efficiency of engineering designers and on-site operation and maintenance. The basic theory of high current bus and engineering electromagnetic field is applied. Based on the principle of hollow current transformers, an equivalent model of GIS shell circulation is established. For steady-state operation of 550 kV GIS and short-circuit fault conditions, circulating currents of shells, short wiring, and grounding wires at different locations are calculated. The circulation and loss distribution rules are given. The calculation results show that when the 550 kV GIS is in steady-state operation, the short-circuit circulating current value at the inlet and outlet ends is greater than other locations; the current value at the fault point near the ground wire is the largest in the fault state; the calculated current of the ground wire and the short wire is greater than the measured value, mainly it is caused by the distribution of grounding resistance. The total loss of GIS system is given through calculation, which gives theoretical guidance for the actual operation of GIS.

Keywords: gas insulate switchgear (GIS); equivalent calculation model; shell circulation; operation loss; operation maintenance and anti-fault measures

(编辑 方晶)

(上接第 200 页)

Thermal runaway characteristic of lithium iron phosphate battery modules through overcharge and the fire extinguishing effect of water mist

ZHAO Lantian¹, JIN Yang¹, ZHAO Zhixing¹, SUN Lei², GUO Dongliang², LIU Yang²

(1. Research Center of Grid Energy Storage and Battery Application School of

Electrical Engineering, Zhengzhou University, Zhengzhou 450001, China;

2. State Grid Jiangsu Electric Power Co., Ltd. Research Institute, Nanjing 211103, China)

Abstract: Thermal runaway and fire extinguishing are both urgent problems in large-scale applications of lithium iron phosphate battery (LFP) modules. In this paper, the thermal runaway characteristic of a single LFP module and a cluster of LFP modules are studied under constant current overcharge mode. Water mist is used as a fire extinguishing agent to study its fire extinguishing effect on single and cluster LFP modules. The experimental results show that the temperatures of the modules in the cluster rise sharply after combustion, with a temperature rise rate of 42.74 °C/s in the first 18 s. The peak temperature is nearly 1 000 °C, which is significantly higher than that of the peak temperature of the single module (600 °C). After 100 seconds of continuous spraying of water mist, the temperatures of all the modules drop rapidly, and the fires are completely extinguished without reignition, thus proving that the fire extinguishing effects by using water mist are satisfactory. Above results provide an effective theoretical and experimental support for the safety and fire extinguishing of the LFP-based energy storage power station.

Keywords: lithium iron phosphate battery; water mist; overcharge; thermal runaway; fire extinguishing

(编辑 方晶)